

Int. J. Electrochem. Sci., 11 (2016) 2982 - 2993

**International Journal of
ELECTROCHEMICAL
SCIENCE**

www.electrochemsci.org

Elemental, Morphological, and Corrosion Characterization of Different Surface States of Co-Cr Alloy for Prosthodontic Applications

Youssef S. Al Jabbari^{1,2,*}, Argiro Ntasi³, Mariana Gaintatzopoulou⁴, Wolf Dieter Mueller⁵, George Eliades³, El-Sayed M. Sherif^{6,7,1}, Spiros Zinelis^{3,1}

¹ Dental Biomaterials Research and Development Chair, College of Dentistry, King Saud University, Riyadh, Saudi Arabia

² Prosthetic Dental Sciences Department, College of Dentistry, King Saud University, Riyadh, Saudi Arabia

³ Department of Biomaterials, School of Dentistry, National and Kapodistrian University of Athens, Athens, Greece

⁴ Department of General & Specialist Dental Practice, College of Dentistry, University of Sharjah, Sharjah, United Arab Emirates

⁵ Dental and Biomaterials Research Group Dental School, "Charite" Medical University of Berlin, Germany

⁶ Center of Excellence for Research in Engineering Materials (CEREM), Advanced Manufacturing Institute, King Saud University, P. O. Box 800, Al-Riyadh 11421, Saudi Arabia

⁷ Electrochemistry and Corrosion Laboratory, Department of Physical Chemistry, National Research Centre (NRC), Dokki, 12622 Cairo, Egypt

*E-mail: yaljabbari@ksu.edu.sa

Received: 22 January 2016 / *Accepted:* 19 February 2016 / *Published:* 1 March 2016

In this study, four different groups were prepared in a cast model of an arch that received four implants made with a Co-Cr dental alloy. The surface of each group was prepared by four different surface treatments, including sandblasting with Al₂O₃ grains (SB), conventional finishing with dental burs (CF), milling with a CAD/CAM device (MIL), and electrodischarge machining (EDM). The characterization of the roughness parameters, morphology, elemental composition, and electrochemical properties of a dental Co-Cr alloy in different surface states exposed to an oral environment were reported. The electrochemical properties were tested with open-circuit potential (OCP) and anodic scan in Ringer's solutions. The results of roughness parameters, elemental composition, OCP, corrosion potential and pitting potential were statistically analyzed by one-way ANOVA and the Tukey-Kramer multiple-comparison test at 95% confidence level. The roughness parameters classified the surfaces from smoothest to roughest according to the following order; CF, MIL, EDM, and SB. The CF group has the best corrosion resistance followed by the EDM, MIL, and SB groups.

Keywords: Co-Cr alloy, corrosion, profilometry, SEM/EDX, surface roughness

1. INTRODUCTION

Dental Co-Cr alloys have been successfully used in the manufacture of a wide range of applications, such as removable partial denture frameworks, fixed porcelain-fused-to-metal restorations, implant-retained meso- and superstructures, etc [1]. Although conventional casting remains the most popular processing technique for these alloys, milling through CAD/CAM technology [2-4] and selective laser sintering (SLM) have been introduced as alternative manufacturing methods [5-7]. Moreover, other techniques— such as Electro-Discharge-Machining (EDM), also known in the dental literature as Spark Erosion— have been recently introduced to improve the passive fitting of implant-retained meso- and superstructures [8-10].

Despite a long and successful record in the dental field, Co-Cr prosthetic device failure is not uncommon in clinical practice [11-13], mostly attributed to fatigue, stress corrosion cracking, stress concentration areas, etc [14-16]. Dental Co-Cr alloys have shown good corrosion resistance in vivo thanks to their passive surface film, but the resistance of this film is dependent on the surface state of the final restoration, including morphological features and/or chemical composition [17-21]. Previous studies have reported that the electrochemical properties of alumina-sandblasted Co-Cr alloys were inferior to those of polished ones [18,19] when tested in fetal bovine serum and Na_2SO_4 . Moreover, the ionic release of a Co-Cr alloy in 0.9% NaCl was higher after alumina sandblasting than after polishing [20]. The latter is a common finding for other types of dental alloys (Type IV Au, Au-Ag-Pd, Ni-Cr, and commercially pure Ti), denoting the significance of surface finishing. In contrast, EDM surfaces of implant superstructures are not directly exposed to oral fluids, but only after loss of epithelial attachment around the implant. In such cases, oral fluid and bacterial penetration into the peri-implant tissue occur [22], triggering electrochemical reactions on metallic surfaces. Although previous studies have shown that sandblasting, polishing, or EDM treatment significantly alters the morphological and/or elemental composition of Co-Cr alloys [21,23-26], the results cannot be directly compared, due to differences in the composition of the alloys tested and in the experimental protocols [18,19,27,28].

Therefore, the aim of this study was a comparative evaluation of the roughness, morphological, elemental, and electrochemical corrosion behavior of a Co-Cr dental alloy after four different surface preparation methods. The null hypothesis was that there are significant differences in the aforementioned properties among the different surface preparation methods.

2. EXPERIMENTAL DETAILS

2.1. Specimen preparation

A completed cast model of an arch that received four dental implants was used for the preparation of nine wax patterns which were invested in a silica-based investment material and cast in

a centrifugal dental device with a dental Co-Cr alloy (Octa C, SAE Dental Products Inc., Bremerhaven, Germany; composition Co, 61.1; Cr, 32.0; Mo, 5.5; Si, <1.0; and Mn, <1.0, all in wt%). The nine cast frameworks were equally divided in three groups SB, CF and EDM. The cast frameworks of first group were cleaned by airborne particle abrasion (110 mesh alumina oxide particles, 0.3 MPa pressure, 45° incidence angle, 10 mm distance), steam-jet treatment, and air-drying (SB treatment). The rest six cast frameworks were conventionally ground and polished with dental burs and polishing instruments (Komet Dental, Gebr. Brasseler GmbH & Co. KG, Lemgo, Germany). The frames were then cleaned with a steam jet and air-dried. Three framework were used as representative of conventional finishing (CF), while the other three were further subjected to an EDM procedure with use of a dental EDM device (EDM 2000, SAE Dental Products Inc., Bremerhaven, Germany), operated with Cu electrodes, 90 V voltage, 0.5-1.5 A current (1.5 A, first and second stages; 0.5 A, final stage), and kerosene as dielectric fluid in all stages.

A stone model of the completed cast model with four implants was prepared by the conventional impression technique, and the stone model was digitized (CAD) with the 3Shape Dental 3D Scanner (R+K CAD/CAM Technologie, Berlin, Germany) and dedicated software (OrganicalMill, R+K CAD/CAM Technologie). The CAD file was used for the fabrication of three milled (MIL) frameworks made of the same dental Co-Cr alloy (Octa C). The milling procedure was performed with the Organical Multi Milling/grinding machine (R+K CAD/CAM Technologie). A brief description of all groups tested is given in Table 1.

Table 1. Brief description of sample preparation of all groups tested.

Groups	Surface preparation method
SB	Airborne aluminum oxide abrasion (110 mesh, 0.3 MPa propulsion pressure, 45° incidence angle, and 10 mm distance)
CF	Conventional finishing after surface grinding and polishing
MIL	Milling with a CAD/CAM dental device
EDM	Electro Discharge Machining with Cu electrodes and kerosene as a dielectric fluid

2.2. Optical profilometry

The specimens were ultrasonically cleaned in acetone for 10 min. Five 3D-surface roughness parameters were evaluated at 12 different regions of the cervical areas (n=12) of each frame work by means of an optical interferometric profiler (Wyko NT1100, Veeco, Tucson, AZ, USA). The experimental conditions were as follows: Mirau lens (20X 2), vertical scanning mode (VSI), 20 µm vertical scan length, and a 113 µm x 148.5 µm analysis area (41.6X magnification), with nominal resolution of 0.1 nm in the z axis and 0.2 µm in the x and y axes. The evaluated surface roughness parameters were reported and defined as the following [28]; S_a is the arithmetic mean deviation (amplitude parameter); S_q is the root mean square roughness (amplitude parameter); S_z is the 10-point

height over the complete surface (amplitude parameter); S_{dr} is the developed interfacial area ratio (developed vs. ideal reference area ratio, (hybrid parameter)); and S_{ci} is the core fluid index (volume that a surface would support from 5-80% of the bearing ratio, (functional parameter)).

2.3. Scanning electron microscopy and energy dispersive X-ray (SEM/EDX) microanalysis

Scanning electron microscopy and energy-dispersive x-ray microanalysis (SEM/EDX) were used to investigate the surface morphology and elemental composition of the groups tested. The frameworks were placed in a SEM (Quanta 200, FEI, Hillsboro, OR, USA), and secondary electron images (SE) were taken from the cervical areas of the frameworks under the following conditions: 20 kV accelerating voltage, 105 μA beam current, and 4536X nominal magnification ($113 \times 113 \mu\text{m}^2$). This magnification was chosen to match the optical profiler of the small side with that of optical profiler 3D images. The elemental composition of each framework was determined from 12 spectra taken from the cervical areas by means of an EDX spectrometer equipped with a super-ultrathin Be window Si(Li) detector (Sapphire, EDAX, Mahwah, NJ, USA). The spectra were collected in area scan mode with 20 kV accelerating voltage, 98 μA beam current, a $53 \times 53 \mu\text{m}^2$ collecting window, 300 s acquisition time, and 30~35% detector dead time. Quantification in wt% was performed by Genesis software (ver 5.1 EDAX) with the ZAF correction method applied in a non-standard analysis mode.

2.4. Electrochemical corrosion testing

The electrochemical properties of different samples were investigated by open-circuit potential (OCP) measurements and anodic scan. The experimental testing was carried out in a Mini Cell System (MCS) connected to a potentiostat (PGC 402 VoltaLab, Radiometer Analytical, Villeurbanne, Cedex, France). A saturated calomel electrode (SCE) and a platinum sheet as were used as reference and counter electrodes, respectively. The effective tip cross-sectional area was 0.008 cm^2 , and a Ringer's solution (Fresenius Kabi, Bad Homburg, Germany; composition, 9.0 g NaCl, 0.24 g $\text{CaCl}_2 \cdot 6\text{H}_2\text{O}$, 0.43 g KCl, 0.2 g NaHCO_3 in 1000 mL distilled water) was used as the test electrolyte. The tip was placed on the cervical areas of samples, and 5 spectra were recorded from each framework, including OCP for 300 s and polarization with potential ranging between -1000 mV and 1250 mV vs. SCE at a 10 mV/s scan rate for both forward and backward directions. All measurements were performed at ambient temperature, and the data were collected with Volta Master software (Radiometer Analytical). From the current-potential curves, the corrosion potential E_{Corr} was determined after Tafel modeling with a 200 mV range for cathodic and anodic branches. Breakdown or pitting potential (E_{Pit}) was also determined from the anodic scan.

2.5. Statistical analysis

The results of roughness parameters, elemental composition, OCP, E_{Corr} and E_{Pit} were statistically analyzed by one-way ANOVA and the Tukey-Kramer multiple-comparison test at an

$\alpha=0.05$ confidence level. Statistical analysis was performed with SigmaStat software (Jandel, St. Raphael, CA, USA).

3. RESULTS

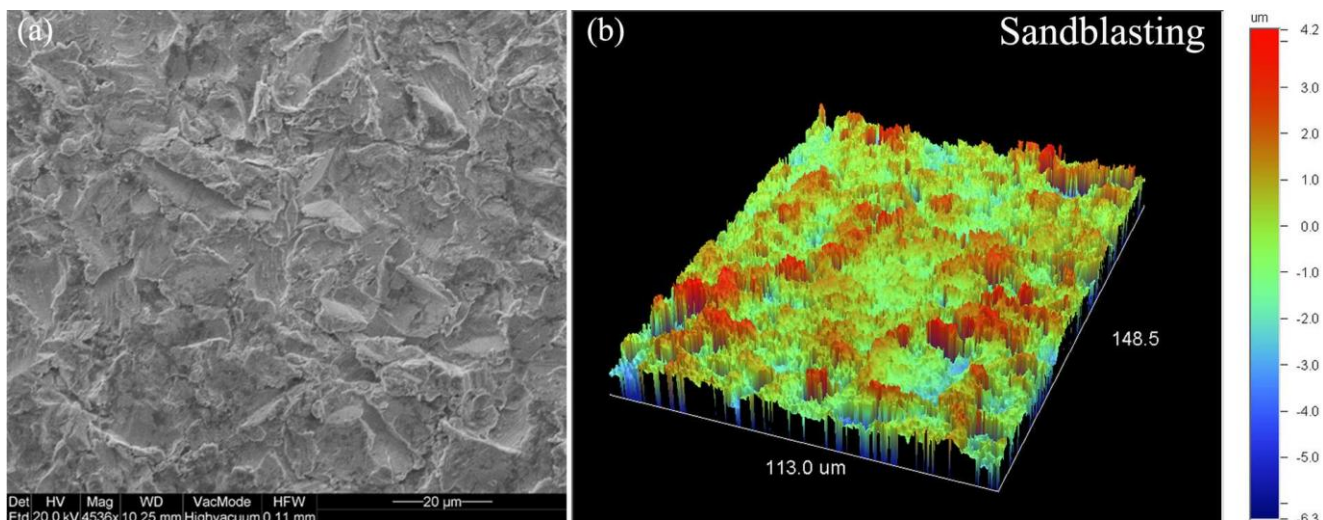


Figure 1. Representative (a) 3D-optical profilometric image along with (b) the corresponding secondary electron image of the sandblasting with Al_2O_3 grains (SB) treatment. The magnification (4536X) of SEI was deliberately chosen to match the size of SEI (110*110 μm) to that of optical profiler 3D image (113X148.5 μm).

The 3D-optical profilometric image and the corresponding secondary electron image of the sandblasting with Al_2O_3 grains (SB) treatment are illustrated in Figure 1.

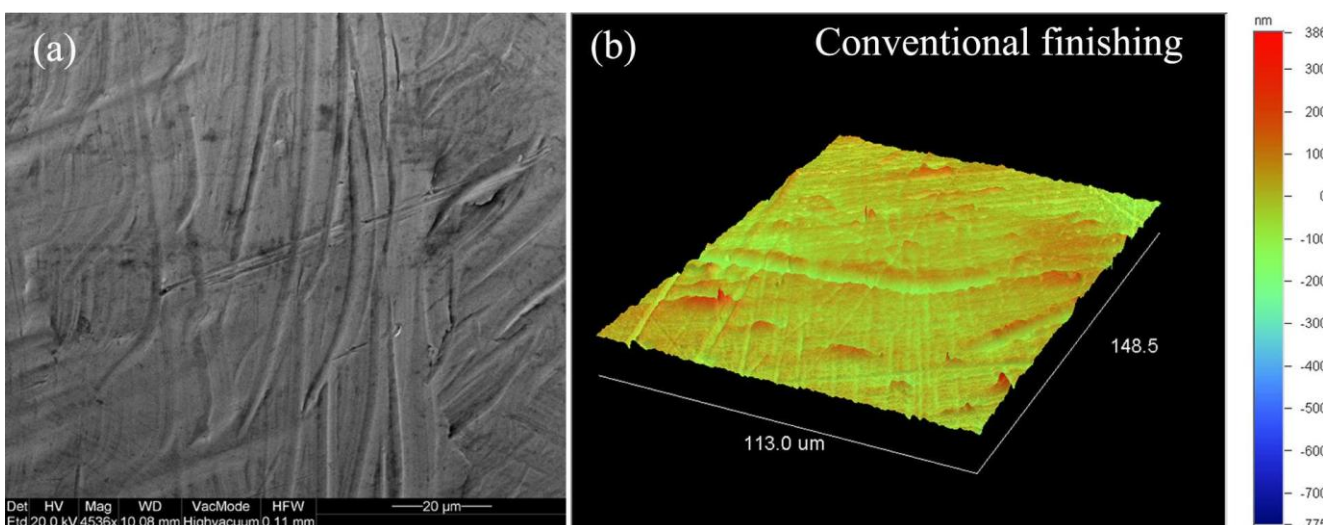


Figure 2. The 3D-optical profilometric image and the corresponding secondary electron image obtained for the conventional finishing with dental burs (CF) treatment. The magnification (4536X) of SEI was deliberately chosen to match the size of SEI (110*110 μm) to that of optical profiler 3D image (113X148.5 μm).

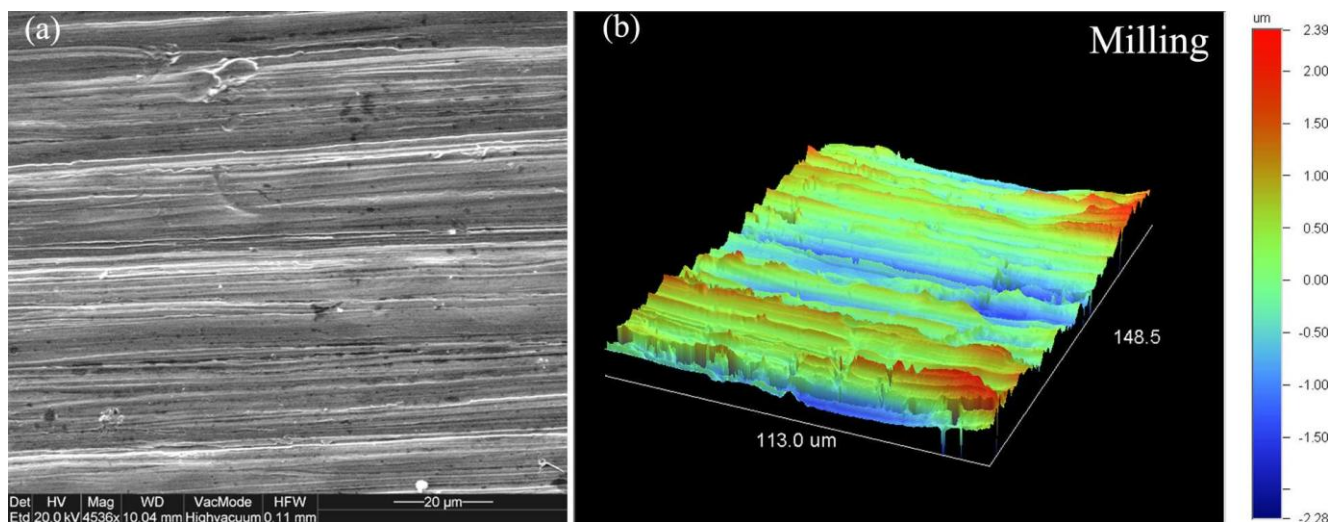


Figure 3. Representative (a) 3D-optical profilometric along with (b) the corresponding secondary electron image for treated sample by milling with a CAD/CAM device (MIL). The magnification (4536X) of SEI was deliberately chosen to match the size of SEI (110*110µm) to that of optical profiler 3D image (113X148.5µm).

The 3D-optical profilometric image and the corresponding secondary electron image for the conventional finishing with dental burs (CF) are also depicted in Figure 2. It is seen from Figure 1 and Figure 2 that the SB treatment demonstrates a random distribution of grooves and peaks with sharp edges, whereas the CF treatment resulted in short, unidirectional, deep surface grooves, with a group of shallower grooves oriented in another direction.

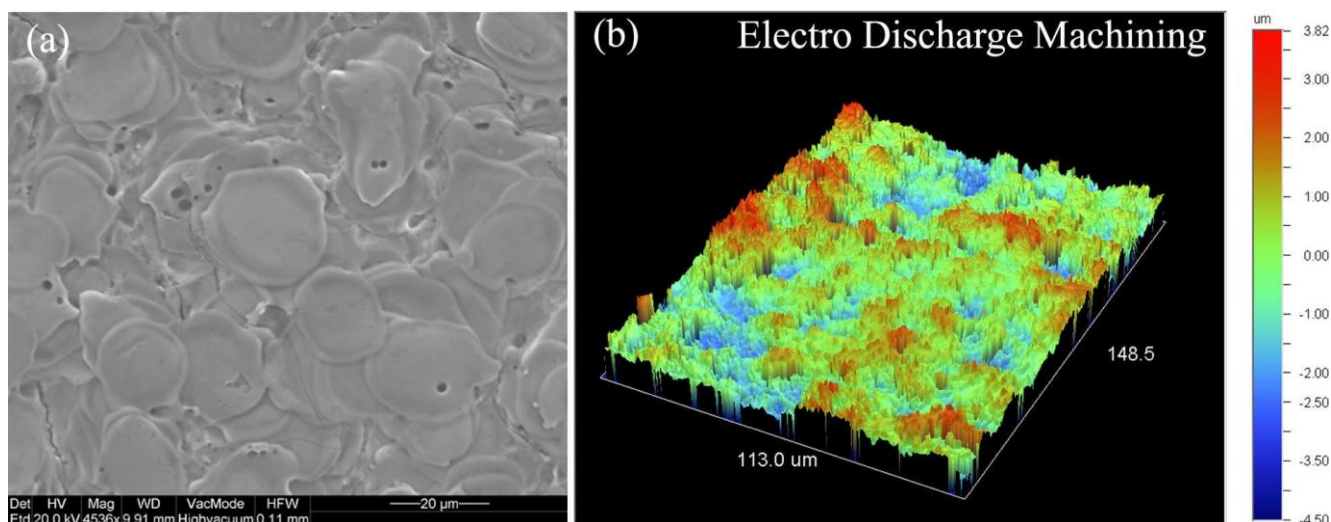


Figure 4. The representative (a) 3D-optical profilometric image and (b) the corresponding secondary electron image for treated sample by electrodischarge machining (EDM). The magnification (4536X) of SEI was deliberately chosen to match the size of SEI (110*110µm) to that of optical profiler 3D image (113X148.5µm).

Figure 3 shows the 3D-optical profilometric image and its corresponding secondary electron image for milling with a CAD/CAM device (MIL), while Figure 4 displays the same images for the electrodischarge machining (EDM). It is noted from Figure 3 and Figure 4 that the MIL treatment resulted in well-oriented parallel striations and machining tracks, contrary to the randomly distributed irregular craters and fissures depicted after EDM treatment.

The results of surface roughness parameters are given in Table 2. For the arithmetic mean deviation (S_a), the root mean square roughness (S_q), the 10-point height over the complete surface (S_z) and the developed interfacial area ratio (S_{dr}) parameters, SB showed the maximum values, followed by EDM, MIL, and CF with statistically significant differences. However, no statistically significant differences were found for the core fluid index (S_{ci}) parameter among the tested groups.

Table 2. Mean values and standard deviations of the tested surface roughness parameters (n=15).

Sample	S_a (nm)	S_q (nm)	S_z (nm)	S_{ci} (nm)	S_{dr} (%)
SB	942±41 ¹	1183±42 ¹	7652±221 ¹	1.42±0.04 ¹	64.8±2.9 ¹
CF	38±6 ²	51±9 ²	423±125 ²	1.39±0.15 ¹	1.4±0.4 ²
MIL	518±67 ³	679±92 ³	3621 ±423 ³	1.37±0.20 ¹	6.3±1.5 ³
EDM	635±23 ⁴	828±42 ⁴	4392±221 ⁴	1.45±0.09 ¹	17.5±2.2 ⁴

Same superscripts denote groups without statistically significant differences per parameter ($p > 0.05$).

Table 3. Quantitative results obtained from the EDX analysis of the different tested groups (n=15).

Element	SB	CF	MIL	EDM
C	2.4±2.0 ¹	0.8±0.1 ¹	0.7±0.3 ¹	14.7±5.2 ²
O	23.1±0.5 ¹	0.8±0.4 ²	0.9±0.2 ²	1.1±0.3 ²
Al	14.9±1.5	ND	ND	ND
Si	2.2±0.4 ¹	0.9±0.5 ²	0.7±0.0 ²	0.7±0.1 ²
Mo	3.8±0.1 ¹	6.2±0.4 ²	6.1±0.3 ²	4.6±0.4 ³
Cr	15.7±0.7 ¹	31.1±0.7 ²	31.0±0.9 ³	23.3±0.9 ⁴
Mn	0.6±0.3 ¹	0.5±0.7 ¹	0.3±0.1 ¹	0.2±0.1 ¹
Fe	0.6±0.3 ¹	0.3±0.2 ¹	0.4±0.1 ¹	0.7±0.3 ¹
Co	33.1±1.0 ¹	60.3±0.2 ²	59.2±0.8 ²	46.9±1.5 ³
Cu	ND	ND	ND	6.7±3.6

ND: Below the detection limit (not detected).

Same superscripts denote groups without statistically significant differences per parameter ($p > 0.05$).

The results of the elemental composition (wt.%) of the alloy surfaces subjected to the various preparation treatments as derived from the EDX analysis are presented in Table 3. Al and Cu were found only on the SB and EDM groups, respectively. The SB group illustrated a significant increase in the oxygen content, while the EDM showed excess in the carbon content. Statistically significant differences were identified for all elements apart from Mn and Fe.

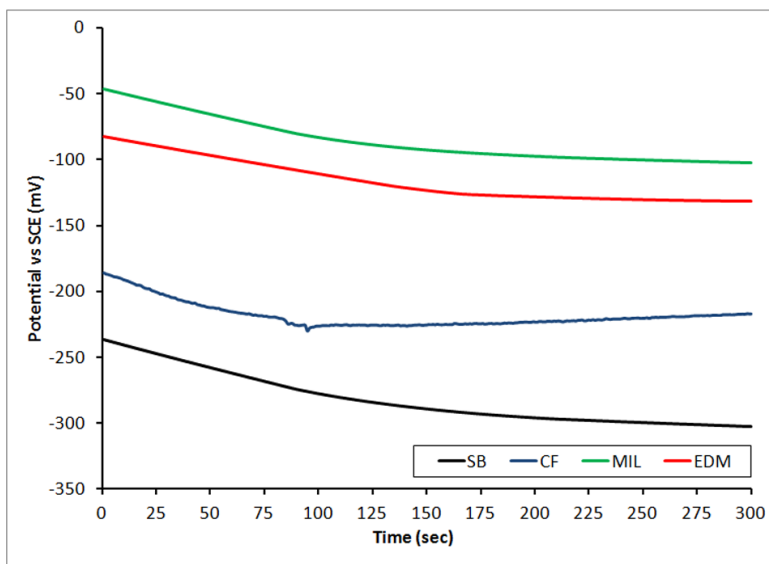


Figure 5. Change of the open-circuit potential with time for SB, CF, MIL, and EDM samples.

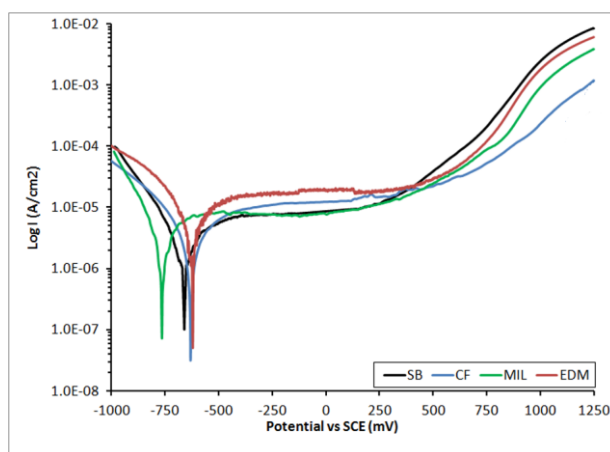


Figure 6. Anodic scan polarization curves obtained for SB, CF, MIL, and EDM tested samples. All materials showed negative hysteresis (shown only in the CF curve for the sake of clarity).

Representative graphs of the electrochemical testing are presented in Figure 5 and Figure 6. The change of the open-circuit potential with time for SB, CF, MIL, and EDM tested samples is displayed in Figure 5. The OCP curves showed a small decrease up to 150 s and then stabilized for the rest of the monitoring time. SB treatment showed the most cathodic OCP values, with significant differences from the rest of the samples. Representative anodic scan curves for all groups are presented

in Figure 6, while the quantitative results are presented in Table 4. The SB and MIL groups demonstrated inferior pitting potential, E_{Pit} .

Table 4. Mean values and standard deviations for OCP, E_{Corr} , E_{Pit} , and types of hysteresis in reverse scans for all groups tested (n=15).

Groups	OCP (mV)	E_{Corr} (mV)	E_{Pit} (mV)
SB	-293±63 ¹	-729±24 ¹	161±37 ¹
CF	-185±40 ²	-708±72 ¹	255±42 ²
MIL	-118±63 ²	-739±75 ¹	152±11 ¹
EDM	-132±47 ²	-675±49 ¹	280±53 ²

Same superscripts denote groups without statistically significant differences per parameter ($p > 0.05$).

4. DISCUSSION

According to the results of this study, the null hypothesis must be accepted, since significant differences were identified in roughness parameters, surface morphology, elemental composition, and electrochemical properties among the various surface preparation methods tested.

The 3D profilometric and secondary electron images (Figure 1 to Figure 4) exhibited the typical patterns of the tested surface treatments. The SB group (Figure 1) exhibited the characteristic valleys due to the pinning action of alumina grains [24]. The CF group (Figure 2) showed groups of two-directional surface grooves, probably attributed to changes in specimen orientation during hand-finishing and the use of polishing burs [23], while parallel serrations in the MIL group (Figure 3) were attributed to machining during the milling of the dental framework from the block. Characteristic patterns with craters in the EDM group (Figure 4) were formed after the collapse of the plasma column (developed between the eroding and working electrodes) and the subsequent re-solidification of the metal atoms [23,30].

Surface roughness parameters were used to quantify the morphological differences among the aforementioned surface textures. Significant differences in S_a , S_q , and S_z values (Table 2) clearly classified the tested surfaces showing that SB is the rougher surface, followed by EDM and MIL, while CF is the smoothest. Despite the diversity in experimental conditions, the results of this study are close to previously reported roughness data for sandblasted ($R_a=990\pm550$ [25], $R_a=1142\pm113$ [31], and $R_a=967\pm263$ [20]) and conventionally finished Co-Cr dental alloys ($R_a=133\pm41$ [32]). The S_{dr} values fit well with the aforementioned classification, since the rougher the surface, the higher the developed area. The results indicate that the developed area for the smoothed CF group is only 1.4% higher than the nominal surface, but 64.7% for the rougher SB group. Despite the differences in

amplitude parameters, no differences were found for core fluid index, S_{ci} , denoting that all surfaces would support the same volume of oral fluids from 5 to 80% of their bearing ratio.

From the standpoint of elemental composition, CF and MIL showed no significant differences (Table 3) apart from Cr content, a finding that might be attributed to different thicknesses of Cr oxide or the possible depletion of Cr in the slag during induction melting in the crucible before casting. The presence of Al and the increase in O and Si content in the SB group are readily explained by the retention of alumina fragments after sandblasting [24,33]. On the contrary, Al has vanished completely from the successive surface treatments in CF and EDM. However, the latter showed the presence of Cu, which is explained by the decomposition of Cu electrodes and increased C content, which is also attributed to the decomposition of the kerosene dielectric fluid in the plasma column during EDM procedures [21,23]. Although EDX analysis is not appropriate for the quantitative analysis of C, especially in a non-standard analysis mode, the results are presented to point out the significant differences in C content among the surfaces tested. This relative C comparison is valid since EDX quantification was subjected to the same matrix effect (the same Co-Cr alloy) and the same acquisition parameters (accelerating voltage, beam current, etc.), without carbon-coating. Previous studies have shown that C is unevenly distributed on the surface, forming Co and Cr carbides [21,34,35].

Electrochemical testing was conducted in a Ringer's solution, extensively used in the relevant literature [21,36-38]. The experimental portion of this study was carried out with the MCS system, since it has the capacity for measurement of irregularly shaped samples (such as full 3D-fidelity dental frameworks) thanks to the small tip surface provided (0.008cm^2). Moreover, the surfaces can be tested exactly as placed in the oral cavity.

OCP curves (Figure 5) showed that the potential of all testing groups was quickly stabilized, after a small reduction of up to about 150 s. SB treatment showed the most cathodic potential, possibly attributed to the very high roughness induced, since sharp peaks increase the tendency of a surface to react due to increased density of dynamic lines. The results of this study fit well with previous data showing that OCP for Co-Cr alloys in Ringer's solution ranged from -300 to -50 mV vs. SCE [36-38].

In accordance with previous studies, E_{Corr} (Figure 6 and Table 4) was found, for sandblasted [20], metallographically polished [20], conventionally finished, and EDM-treated surfaces [21]. However, E_{Pit} was higher for CF-treated surface and EDM-treated surface in comparison with SB and MIL, indicating that the passive region was inferior for the latter. An explanation for SB performance could be the very rough surface and the fact that the implanted alumina fragments disrupted the protective oxide layer. A third possible mechanism could be the residual stresses developed at the subsurface layers of the material after sandblasting [39,40], which facilitate oxide film degradation. Residual stresses due to thermal phenomena during cutting are the only possible explanation for the lower pitting potential observed in the MIL treatment, although it must also be noted that the microstructure of the prefabricated Co-Cr block [41] is quite different from that of cast material, and this might have an effect as well. Despite the morphological and elemental differences induced by EDM, no differences were found in the electrochemical parameters with CF. The results of OCP and polarization advocate SB as the less-corrosion-resistant surface, since it combines the most cathodic OCP potential and lower pitting potential, followed by MIL and EDM, whereas CF demonstrated the best properties. This finding is in accordance with reports from previous studies [18,19].

The results of this study show that the electrochemical properties of the Co-Cr alloy are dependent on the roughness and elemental differences among different surface treatments. The biggest difference in OCP potential is between SB and MIL (differences in mean values = 176 mV), which is marginally less than the 200 mV threshold for galvanic action. Therefore, it might be concluded that in the experimental conditions of this study, galvanic action is not anticipated in clinical conditions among the different surface treatments. However, the dental technician and dentist should be aware that the sandblasting texture must be eliminated during the preparation procedure, especially in the case of removable dentures, where large and irregular metallic surfaces are exposed to oral fluids. The different surface preparation treatments tested showed great differences in all properties tested, and therefore differences in their clinical behavior are anticipated.

5. CONCLUSIONS

The preparation, elemental, morphological and corrosion characterization of four different surface treatments of implants made with a Co-Cr dental alloy, namely; SB, CF, MIL and EDM were reported. The 3D profilometric and secondary electron images for the different surface finished samples proved that each group has a different pattern. The surface roughness parameters (S_a , S_q , and S_z) indicated that there is a significant difference of the tested surface and that SB is the roughest surface, followed by EDM and MIL, while CF is the smoothest. The elemental composition test showed that both CF and MIL had no significant differences in compositions, while SB displayed the presence of Al and an increased content for O and Si. The OCP measurements of the different samples after their immersion in a Ringer's solution revealed that the value of the steady state potential shifts towards the less negative direction in the following order SB < CF < EDM < MIL. The anodic scan showed that CF combines the highest corrosion resistance characteristics. Within the limitations of this experimental study it can be said that these different finishing methods have a significant effect on morphology, elemental composition and electrochemical corrosion behavior of the investigated Co-Cr alloy.

ACKNOWLEDGEMENTS

This study was funded by a research grant (RGP-VPP-206) from the Research Group Program, Deanship of Scientific Research, King Saud University, Riyadh, Saudi Arabia.

References

1. J.C. Wataha, *J. Prosthet. Dent.*, 87 (2002) 351.
2. L. Hjalmarsson, A. Ortorp, J.I. Smedberg, T. Jemt, *Clin. Implant Dent. Relat. Res.*, 12 (2010) 271.
3. S. Witkowski, F. Komine, T. Gerds, *J. Prosthet. Dent.*, 96 (2006) 47.
4. J. Willer, A. Rossbach, H.P. Weber, *J. Prosthet. Dent.*, 80 (1998) 346.
5. R. van Noort, *Dent. Mater.*, 28 (2012) 3.
6. X.W. Ren, L. Zeng, Z.M. Wei, X.Z. Xin, B. Wei, *J. Prosthet. Dent.*, 115 (2016) 109.
7. K. Quante, K. Ludwig, M. Kern, *Dent. Mater.*, 24 (2008) 1311.
8. A.D. Linehan, A.S. Windeler, *J. Prosthodont.*, 3 (1994) 88.

9. I.A. Sartori, R.F. Ribeiro, C.E. Francischone, Mda G. de Mattos, *J. Prosthet. Dent.*, 92 (2004) 132.
10. G.G. Romero, R. Engelmeier, J.M. Powers, A.A. Canterbury, *J. Prosthet. Dent.*, 84 (2000) 602.
11. A. Ortorp, A. Ascher, P.A Svanborg, *Int. J. Prosthodont.*, 25 (2012) 480.
12. Stavros A. Yannikakis, Alcibiades J.Zissis, Gregory L. Polyzois, *Quintessence of Dental Technology*, 23 (2000) 184.
13. H.A. Vermeulen, H.M. Keltjens, M.A. van't Hof, A.F. Kayser, *J. Prosthet. Dent.* 76 (1996) 267.
14. J.F. Bates, *Br. Dent. J.*, 120 (1966) 79.
15. R. van Noort, D.J. Lamb, *J. Dent.*, 12 (1984) 122.
16. L.V. Lassila, P.K. Vallittu, *J. Prosthet. Dent.*, 80 (1998) 708.
17. B.G. Pound, *J. Biomed. Mater. Res. A*, 94 (2010) 93.
18. F. Contu, B. Elsener, H. Bohni, *J. Biomed. Mater. Res. A*, 62 (2002) 412.
19. F. Contu, B. Elsener, H. Bohni, *J. Biomed. Mater. Res. A*, 67 (2003) 246.
20. T. Kaneko, M. Hattori, K. Hasegawa, M. Yoshinari, E. Kawada, Y. Oda, *Bull. Tokyo Dent. Coll.*, 41 (2000) 49.
21. A. Ntasi, W.D. Mueller, G. Eliades, S. Zinelis, *Dent. Mater.*, 26 (2010) e237.
22. T. Berglundh, J. Lindhe, C. Marinello, I. Ericsson, B. Liljenberg, *Clin. Oral. Implants Res.*, 3 (1992) 1.
23. S. Zinelis, *Dent. Mater.*, 23 (2007) 601.
24. Y.S. Al Jabbari, S. Zinelis, G. Eliades, *Dent. Mater. J.*, 31 (2012) 249.
25. R. Castillo-Oyague, R. Osorio, E. Osorio, F. Sanchez-Aguilera, M. Toledano, *Microsc. Res. Tech.*, 75 (2012) 1206.
26. S. Hama Suleiman, P. Vult von Steyern, *Acta Odontol. Scand.*, 71 (2013) 1280.
27. J. Qiu, W.Q. Yu, F.Q. Zhang, R.J. Smales, Y.L. Zhang, C.H. Lu, *Eur. J. Oral. Sci.*, 119 (2011) 93.
28. R. Galo, R.F. Ribeiro RF, R.C. Rodrigues, L.A. Rocha, G. de Mattos Mda, *Braz. Dent. J.*, 23 (2012) 141.
29. E. Gadelmawla, M. Koura, T. Maksoud, I. Elewa, H. Soliman, *J. Mater. Process Technol.*, 123 (2002) 133.
30. A. Acar, O. Inan, S. Halkaci, *J. Biomed. Mater. Res. B Appl. Biomater.*, 82 (2007) 267.
31. Y. Taga, K. Kawai, T. Nokubi, *J. Prosthet. Dent.*, 85 (2001) 357.
32. K.S. Jang, S.J. Youn, Y.S. Kim, *J. Prosthet. Dent.*, 86 (2001) 93.
33. M. Kern, V.P. Thompson, *Dent. Mater.*, 9 (1993) 151.
34. S. Kumar, R. Singh, T.P. Singh, B.L. Sethi, *J. Mater. Process Tech.*, 209 (2009) 3675.
35. G. Cusanelli, A. Hessler-Wyser, F. Bobard, R. Demellayer, R. Perez, R. Flukige, *J. Mater. Process Tech.*, 149 (2004) 289.
36. E. Angelini, M. Pezzoli, F. Rosalbino, F., Zucchi, *J. Dent.*, 19 (1991) 56.
37. P. Battaini, *La Metallurgia Italiana*, Vol. 2000, issue 6 (2000) 27-34.
38. J. Hubrecht, Electrochemical impedance spectroscopy as a surface analytical technique for biomaterials. In: J. Helsen, J. Breme, editors, *Metals as Biomaterials*, New York: John Wiley & Sons, p. 405-66 (1988).
39. M.J. Reyes, Y. Oshida, C.J. Andres, T. Barco, S. Hovijitra, D. Brown, *Biomed. Mater. Eng.*, 11 (2001) 117.
40. Z. Cai, N. Bunce, M.E. Nunn, T. Okabe, *Biomaterials*, 22 (2001) 979.
41. B. Karpuschewski, H.J. Pieper, M. Krause, J. Doring, CoCr Is Not the Same: CoCr-Blanks for Dental Machining. In: Schuh Günther, Neugebauer Reimund, E. Uhlmann, editors, *Future Trends in Production Engineering*, Springer-Verlag Berlin Heidelberg, p. 261-74 (2013).